

Article

Spongenolactones A–C, Bioactive 5,5,6,6,5-Pentacyclic Spongian Diterpenes from the Red Sea Sponge *Spongia* sp.

Chi-Jen Tai ¹, Atallah F. Ahmed ^{2,3} , Chih-Hua Chao ^{4,5} , Chia-Hung Yen ^{6,7} , Tsong-Long Hwang ^{8,9,10} , Fang-Rong Chang ⁶ , Yusheng M. Huang ^{11,12}  and Jyh-Horng Sheu ^{1,6,13,14,*}

- ¹ Doctoral Degree Program in Marine Biotechnology, National Sun Yat-sen University, Kaohsiung 80424, Taiwan; d035620001@nssysu.edu.tw
- ² Department of Pharmacognosy, College of Pharmacy, King Saud University, Riyadh 11451, Saudi Arabia; afahmed@ksu.edu.sa
- ³ Department of Pharmacognosy, Faculty of Pharmacy, Mansoura University, Mansoura 35516, Egypt
- ⁴ School of Pharmacy, China Medical University, Taichung 40604, Taiwan; chchao@mail.cmu.edu.tw
- ⁵ Chinese Medicine Research and Development Center, China Medical University Hospital, Taichung 40604, Taiwan
- ⁶ Graduate Institute of Natural Products, College of Pharmacy, Kaohsiung Medical University, Kaohsiung 80708, Taiwan; chyen@kmu.edu.tw (C.-H.Y.); aaronfrc@kmu.edu.tw (F.-R.C.)
- ⁷ National Natural Product Libraries and High-Throughput Screening Core Facility, Kaohsiung Medical University, Kaohsiung 80708, Taiwan
- ⁸ Graduate Institute of Natural Products, College of Medicine, Chang Gung University, Taoyuan 333, Taiwan; htl@mail.cgu.edu.tw
- ⁹ Research Center for Chinese Herbal Medicine, Graduate Institute of Healthy Industry Technology, College of Human Ecology, Chang Gung University of Science and Technology, Taoyuan 33303, Taiwan
- ¹⁰ Department of Anesthesiology, Chang Gung Memorial Hospital, Taoyuan 333423, Taiwan
- ¹¹ Department of Marine Recreation, National Penghu University of Science and Technology, Magong, Penghu 88046, Taiwan; yusheng@gms.npu.edu.tw
- ¹² Tropical Island Sustainable Development Research Center, National Penghu University of Science and Technology, Magong, Penghu 88046, Taiwan
- ¹³ Department of Marine Biotechnology and Resources, National Sun Yat-sen University, Kaohsiung 80424, Taiwan
- ¹⁴ Department of Medical Research, China Medical University Hospital, China Medical University, Taichung 404333, Taiwan
- * Correspondence: sheu@mail.nssysu.edu.tw; Tel.: +886-7-525-2000 (ext. 5030); Fax: +886-7-525-5020



Citation: Tai, C.-J.; Ahmed, A.F.; Chao, C.-H.; Yen, C.-H.; Hwang, T.-L.; Chang, F.-R.; Huang, Y.M.; Sheu, J.-H. Spongenolactones A–C, Bioactive 5,5,6,6,5-Pentacyclic Spongian Diterpenes from the Red Sea Sponge *Spongia* sp. *Mar. Drugs* **2022**, *20*, 498. <https://doi.org/10.3390/md20080498>

Academic Editor: Efstathia Ioannou

Received: 28 June 2022

Accepted: 29 July 2022

Published: 1 August 2022

Publisher's Note: MDPI stays neutral with regard to jurisdictional claims in published maps and institutional affiliations.



Copyright: © 2022 by the authors. Licensee MDPI, Basel, Switzerland. This article is an open access article distributed under the terms and conditions of the Creative Commons Attribution (CC BY) license (<https://creativecommons.org/licenses/by/4.0/>).

Abstract: Three new 5,5,6,6,5-pentacyclic spongian diterpenes, spongenolactones A–C (1–3), were isolated from a Red Sea sponge *Spongia* sp. The structures of the new metabolites were elucidated by extensive spectroscopic analysis and the absolute configurations of 1–3 were determined on the basis of comparison of the experimental circular dichroism (CD) and calculated electronic circular dichroism (ECD) spectra. Compounds 1–3 are the first 5,5,6,6,5-pentacyclic spongian diterpenes bearing an β -hydroxy group at C-1. These metabolites were assayed for their cytotoxic, antibacterial, and anti-inflammatory activities. All three compounds were found to exert inhibitory activity against superoxide anion generation in fMLF/CB-stimulated human neutrophils. Furthermore, 1 showed a higher activity against the growth of *Staphylococcus aureus* in comparison to 2.

Keywords: Red Sea sponge; *Spongia* sp.; 5,5,6,6,5-pentacyclic spongian diterpenes; anti-inflammatory assay; antibacterial assay

1. Introduction

Sponges of the genus *Spongia* have been proven to be rich sources of structurally diversified secondary metabolites [1,2]. A series of previous studies for the discovery of versatile molecular structures and bioactivities of compounds from sponges of the genus *Spongia* have been reported [3–11]. Our recent investigation on the secondary metabolites of a Red Sea sponge *Spongia* sp. has led to the isolation of a series of diverse new natural products,

including a 5,5,6,6,5-pentacyclic diterpenoid, two furanotrinorsesquiterpenoid acids, a furanyl trinorsesquiterpenoid, a halogenated and oxygenated labdane, a highly oxygenated steroid, a steroid with the rare seven-membered lactone B ring, and an α,β -unsaturated fatty acid [12,13]. In our continuing effort to discover new metabolites from this sponge *Spongia* sp., we have further discovered three new diterpenes with 5,5,6,6,5-pentacyclic structures (5,6,6-tricarbocyclic ones with two five-membered lactones), spongenolactones A–C (1–3) (Figure 1). The molecular structures of 1–3 were established by detailed analysis of MS, IR, and NMR spectra (Supplementary Figures S1–S26), and by comparison of their NMR spectral data with those of structurally related known compounds. Further, the absolute configurations of 1–3 were determined by comparison of the experimental CD and calculated ECD spectra. Moreover, the cytotoxic activity of compounds 1–3 toward human hepatocellular carcinoma (HCC) Huh 7 cell line, their antibacterial activity against the growth of *Staphylococcus aureus*, and their anti-inflammatory activity toward the inhibition of the superoxide anion generation and elastase release in *N*-formyl-methionyl-leucyl phenylalanine/cytochalasin B (fMLF/CB)-induced human neutrophils, were also evaluated.

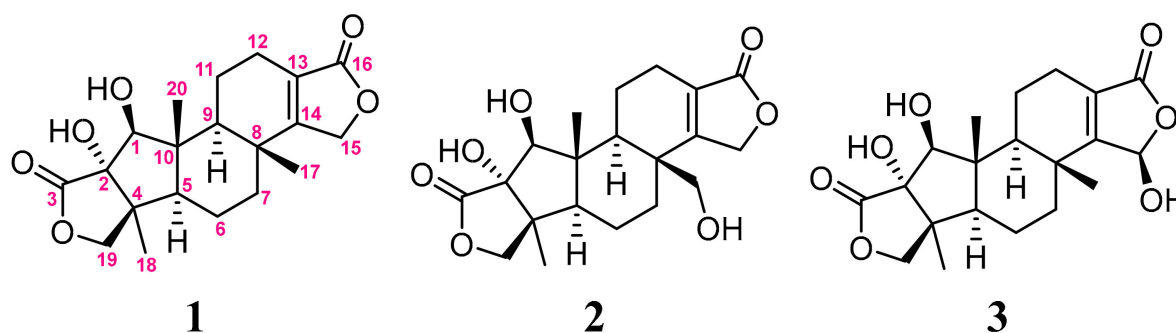


Figure 1. Structures of metabolites 1–3.

2. Results and Discussion

The sample of *Spongia* sp., collected off the Red Sea coast of Jeddah, Saudi Arabia, in 2016, was freeze-dried. The lyophilized sample (550 g) was chopped and extracted with EtOAc/MeOH/CH₂Cl₂. The crude extract was partitioned in water with CH₂Cl₂ to obtain the CH₂Cl₂ fraction (18.47 g), which was subjected to repeated column chromatography and high performance liquid chromatography (HPLC) to afford compounds 1 (2.4 mg), 2 (2.0 mg), and 3 (3.5 mg) (Figure 1).

Compound 1 was isolated as a white powder. The HRESIMS of 1 (m/z 385.1623 [M + Na]⁺, calcd for C₂₀H₂₆O₆Na, 385.1622, Supplementary Figure S1) revealed a molecular formula of C₂₀H₂₆O₆, implying eight degrees of unsaturation. The IR spectrum of 1 showed the presence of hydroxy, carbonyl, and olefinic functionalities as revealed from the absorptions at 3444, 1747, 1683, and 1653 cm⁻¹, respectively. The ¹³C NMR spectroscopic data of 1 showed 20 carbon signals (Table 1 and Supplementary Figure S3), which were assigned with the assistance of the DEPT spectrum into three methyls (δ_C 22.4, 22.4, and 15.6); six methylenes (δ_C 38.3, 22.2, 19.9, 18.6, including two oxygenated methylenes at δ_C 75.3 and 68.8); three methines (δ_C 56.1, 49.4, including one oxygenated methine at δ_C 91.2); and eight quaternary carbons (δ_C 183.3, 174.7, 172.2, 123.5, 90.2, 48.6, 47.4, and 38.0). In total, the NMR spectroscopic data of 1 (Table 1) displayed signals for an α -hydroxy- γ -lactone (δ_C 183.3 C, 90.2 C, 75.3 CH₂, and 48.6 C; δ_H 4.40 and 3.83, each 1H, d, J = 10.0 Hz,) [12] and an unsaturated γ -lactone (δ_C 174.7 C, 172.2 C, 123.5 C, and 68.8 CH₂; δ_H 4.82, 1H, tt, J = 17.0, 2.5 Hz and 4.51, 1H, dd, J = 17.0, 2.5 Hz) [14,15]. Further, the ¹H–¹H COSY experiment revealed the presence of two partial structures (Figure 2), which were connected by the HMBC correlations of 1 (Figure 2) to establish the 5,5,6,6,5-pentacyclic structure of 1 [3,4,12].

Table 1. ^{13}C and ^1H NMR data for compounds 1–3 ^a.

	1		2		3	
Position	δ_{H}	δ_{C}	δ_{H}	δ_{C}	δ_{H}	δ_{C}
1	3.86, br s	91.2, CH	3.84 br s	91.1, CH	3.83, br s	91.2, CH ₂
2	—	90.2, C	—	90.1, C	—	90.4, C
3	—	183.3, C	—	182.4, C	—	183.3, C
4	—	48.6, C	—	48.6, C	—	48.7, C
5	2.00, dd (13.0, 1.5) ^b	56.1, CH	2.01, m	56.2, CH	1.96, m	56.1, CH
6 α	1.60, m	18.6, CH ₂	1.57 m	18.4, CH ₂	1.61, m	18.4, CH ₂
6 β	1.75, m		1.71 dd (13.0, 3.0)		1.74, m	
7 α	1.22, m	38.3, CH ₂	1.03 dt (13.0, 3.5)	33.2, CH ₂	1.14, m	37.8, CH ₂
7 β	1.81, m		2.23 m		1.98, m	
8	—	38.0, C	—	44.2, C	—	38.1, C
9	1.88, dd (12.0, 1.0)	49.4, CH	1.93, dd (12.0, 2.0)	49.9, CH	1.74, m	50.0, CH
10	—	47.4, C	—	47.1, C	—	47.5, C
11 α	1.79, m	19.9, CH ₂	1.76, m	19.5, CH ₂	1.77, m	19.8, CH ₂
11 β	1.65, m		1.82, m		1.66, m	
12 α	2.02, m	22.2, CH ₂	2.04 m	22.2, CH ₂	2.03, m	22.1, CH ₂
12 β	2.22, m		2.24 m		2.26, m	
13	—	123.5, C	—	124.9, C	—	127.8, C
14	—	172.2, C	—	170.5, C	—	169.0, C
15 α	4.51, dd (17.0, 2.5)	68.8, CH ₂	4.53, dd (17.0, 2.5)	72.4, CH ₂	5.86, d (2.0)	97.7, CH
15 β	4.82, tt (17.0, 2.5)		4.96, tt (17.0, 2.5)			
16	—	174.7, C	—	174.8, C	—	172.9, C
17	1.19, s	22.4, CH ₃	3.67, dd (10.5, 4.5) 4.01, dd (10.5, 4.5)	65.3, CH ₂	1.26, s	21.0, CH ₃
18	1.13, s	22.4, CH ₃	1.12, s	22.4, CH ₃	1.14, s	22.4, CH ₃
19 α	3.83, d (10.0)	75.3, CH ₂	3.82, d (10.0)	75.3, CH ₂	3.83, d (10.0)	75.4, CH ₂
19 β	4.40, d (10.0)		4.40, d (10.0)		4.40, d (10.0)	
20	0.80, s	15.6, CH ₃	0.76, s	15.6, CH ₃	0.80, s	15.8, CH ₃

^a ^{13}C and ^1H spectra recorded at 125 and 500 MHz in acetone-*d*₆; ^b *J* values (Hz) in parentheses.

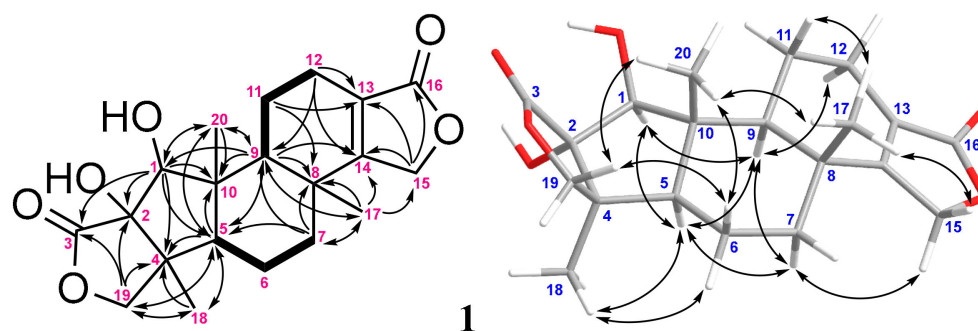


Figure 2. The selected COSY (■), HMBC (→), and key NOESY (↔) correlations of **1**.

In the NOESY spectrum of **1**, the NOE interactions (Figure 2) of H₃-20 with both H₃-17 and one proton (δ_{H} 4.40) of H₂-19, of H₃-17 with one proton (δ_{H} 4.82) of H₂-15 and of the proton at δ_{H} 4.40 of H₂-19 with one proton (δ_{H} 1.75) at C-6 suggested that these protons should be positioned on the same plane, and were all assumed as β protons. By contrast, the correlations of H-6 α (δ_{H} 1.60) with H₃-18, of H₃-18 with H-5, of H-5 with both H-7 α (δ_{H} 1.22) and H-9, of H-7 α with both H-9 and H-15 α (δ_{H} 4.51); and of H-1 with both H-5 and H-9, revealed that these protons should be located on the same side, and were all assumed to be α -oriented. Further, the absolute configuration of **1** was determined by the comparison of the experimental CD and the calculated ECD spectra (Figure 3). The ECD curves of 1*S*,2*S*,4*S*,5*R*,8*R*,9*S*,10*R*-**1** (**1a**) and its enantiomer 1*R*,2*R*,4*R*,5*S*,8*S*,9*R*,10*S*-**1** (**1b**) were calculated at the CAM-B3LYP/6-311+G (d,p) level of theory, including an IEFPCM solvent model for MeOH, by the Gaussian 9.0 program [16,17]. The CD spectrum of **1**

(Figure 3) showed positive and negative Cotton effects at 214.5 and 234.0 nm, respectively, which was found to be well consistent with the calculated ECD of **1a** (212.5 and 230.4 nm, Figure 3), and the absolute configuration of **1** was thus elucidated as 1*S*,2*R*,4*S*,5*R*,8*R*,9*S*, and 10*R*. Based on the above observations, the structure of **1** was identified as a new compound possessing the recently discovered 5,5,6,6,5-pentacyclic-based skeleton [3,4,12], but with a characteristic 1β-OH and named spongenolactone A.

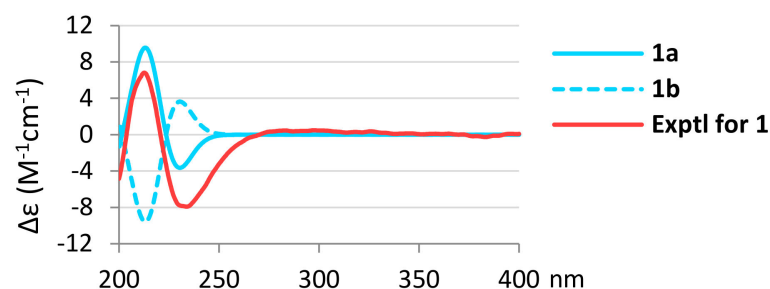


Figure 3. Calculated ECD curves of 1*S*,2*S*,4*S*,5*R*,8*R*,9*S*,10*R*-**1** (**1a**) and 1*R*,2*R*,4*R*,5*S*,8*S*,9*R*,10*S*-**1** (**1b**), and the experimental CD curve of **1**.

The ¹H and ¹³C NMR data of metabolite **2** were very similar to those of **1** (Table 1), with the exception that the methyl group (δ_{H} 1.19, s, 3H and δ_{C} 22.4, CH₃) at C-8 in **1** was oxidized to a hydroxymethyl (δ_{H} 3.67 and 4.01, both dd, $J = 10.5, 4.5, 1\text{H}$; δ_{C} 65.3, CH₂) in **2**. The extensive analyses of COSY, HMBC, and NOESY 2D NMR experiments further confirmed that **2** is the 17-oxygenated derivative of **1** (Figure 4).

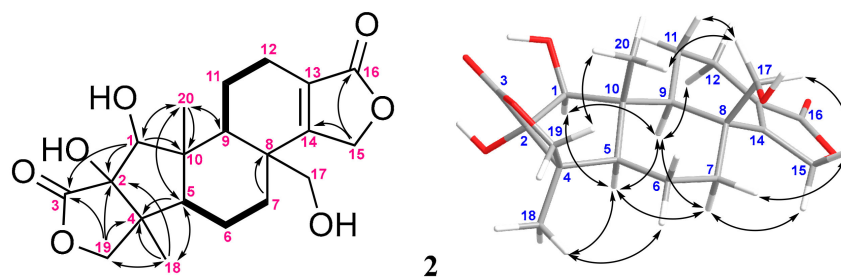


Figure 4. The selected COSY (■), HMBC (→), and key NOESY (↔) correlations of **2**.

The ¹H and ¹³C NMR data of compound **3** were also very similar to those of **1** (Table 1), except that the methylene group (δ_{H} 4.82, 1H, tt, $J = 17.0, 2.5$ Hz and 4.51, 1H, dd, $J = 17.0, 2.5$ Hz; δ_{C} 68.8, CH₂) in the γ -lactone of **1** was converted to an acetal (δ_{H} 5.86, d, $J = 2.0$ Hz, 1H; δ_{C} 97.7, CH) in **3** (Figure 5). The detailed analyses of HMBC correlations (Figures 5 and S24) confirmed that **3** is a 15-hydroxylated derivative of **1**. Furthermore, except for H-15 of **3**, which was observed not to exhibit any NOE interaction with other protons, the NOESY correlations (Figure 5) established the 1*S**,2*S**,4*S**,5*R**,8*R**,9*S**, and 10*R** relative configuration of **3**.

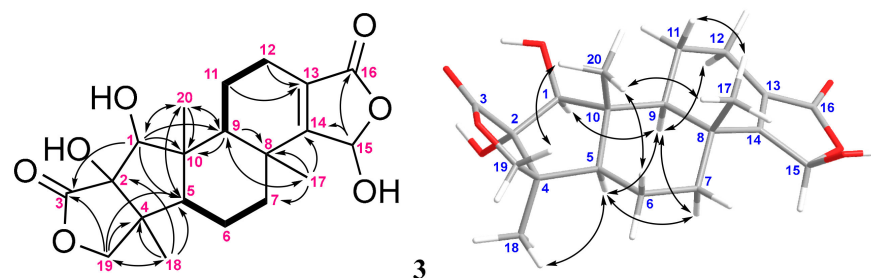


Figure 5. The selected COSY (■), HMBC (→), and key NOESY (↔) correlations of **3**.

Further, the absolute configuration of **2** was also elucidated by the comparison of the experimental CD and calculated ECD spectra (Figure 6a). The calculated ECD spectra of 1*S*,2*S*,4*S*,5*R*,8*R*,9*S*,10*R*-**2** (**2a**) and its enantiomer 1*R*,2*R*,4*R*,5*S*,8*S*,9*R*,10*S*-**2** (**2b**) were also obtained at the CAM-B3LYP/6-311+G (d,p) level of theory by the Gaussian 9.0 program. The CD spectrum of **2** (Figure 6a) showed positive and negative Cotton effects at 211.0 and 231.0 nm, respectively, which was found to match well with the calculated ECD of **2a**, which also showed corresponding positive and negative Cotton effects at 211.2 and 229.9 nm (Figure 6a). The absolute configuration of **2** was thus established as 1*S*,2*S*,4*S*,5*R*,8*R*,9*S*, and 10*R*. Moreover, the absolute stereochemistry of **3**, including the configuration of C-15, was elucidated to be that of **3a** (1*S*,2*S*,4*S*,5*R*,8*R*,9*S*,10*R*,15*R*) rather than that of the enantiomer **3b** (1*R*,2*R*,4*R*,5*S*,8*S*,9*R*,10*S*,15*S*) and the 15-epimer **3c** with a (1*S*,2*S*,4*S*,5*R*,8*R*,9*S*,10*R*,15*S*)-configuration (Figure 6b). Based on the above results, the structures of metabolites **2** and **3** were fully determined, and named spongenolactones B and C, respectively.

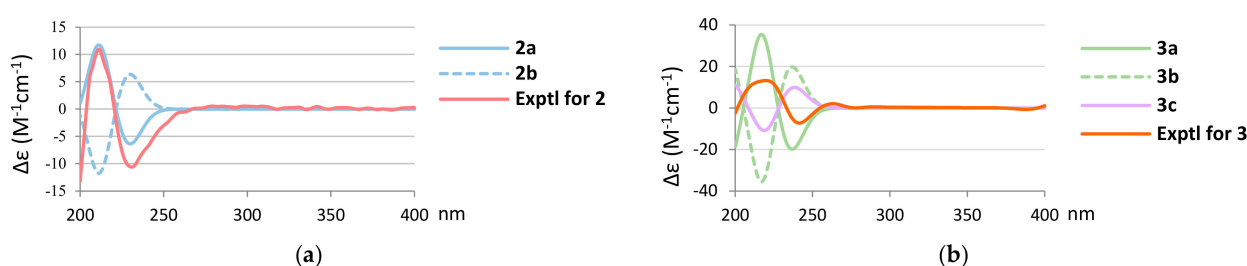


Figure 6. (a) Calculated ECD curves of 1*S*,2*S*,4*S*,5*R*,8*R*,9*S*,10*R*-**2** (**2a**), 1*R*,2*R*,4*R*,5*S*,8*S*,9*R*,10*S*-**2** (**2b**), and the experimental CD curve of **2**. (b) Calculated ECD curves of 1*S*,2*S*,4*S*,5*R*,8*R*,9*S*,10*R*,15*R*-**3** (**3a**), 1*R*,2*R*,4*R*,5*S*,8*S*,9*R*,10*S*,15*S*-**3** (**3b**), 1*S*,2*S*,4*S*,5*R*,8*R*,9*S*,10*R*,15*S*-**3** (**3c**), and the experimental CD curve of **3**.

In order to discover the biological activity of new metabolites for future medicinal applications, **1–3** were tested for their cytotoxic, antibacterial, and anti-inflammatory activities. The cytotoxicity of **1–3** against HCC Huh7 cell line was evaluated by the resazurin assay [18,19], and none of the compounds showed notable activity against the growth of this cancer cell line. Furthermore, the assay for the growth inhibition of *S. aureus* showed that compound **1** exhibited 46%, 47%, and 93% inhibition at 50, 100, and 200 μ M, respectively, while **2** displayed 24%, 42%, and 40% inhibition at 50, 100, and 200 μ M, respectively.

The in vitro anti-inflammatory effects of **1–3** were also evaluated. At a concentration of 20 μ M, compounds **1–3** displayed anti-inflammatory activity in suppressing the generation of superoxide anion ($O_2^{\cdot-}$) and the elastase release, relative to the corresponding values of the control cells stimulated with fMLF/CB (Table 2) [20–22]. At 20 μ M, **1–3** exhibited inhibitory activity against the generation of superoxide anion ($61.0 \pm 4.4\%$, $70.8 \pm 4.8\%$, and $58.9 \pm 6.0\%$, respectively) with IC_{50} values of 16.5 ± 1.6 , 13.1 ± 1.3 , and 17.4 ± 1.9 μ M, respectively. Furthermore, **2** displayed an inhibitory activity against elastase release ($52.2 \pm 1.4\%$) at 20 μ M with IC_{50} values of 18.6 ± 0.9 μ M. Metabolites **1** and **3** also showed inhibitory activity against elastase release ($49.8 \pm 4.2\%$ and $46.5 \pm 6.2\%$, respectively).

Table 2. Inhibitory effects of compounds **1–3** on superoxide anion generation and elastase release by human neutrophils.

Compound	Superoxide Anion		Elastase Release	
	IC_{50} (μ M) ^a	Inh% ^b	IC_{50} (μ M)	Inh%
1	16.5 ± 1.6	61.0 ± 4.4 ***	>20	49.8 ± 4.2 ***
2	13.1 ± 1.3	70.8 ± 4.8 ***	18.6 ± 0.9	52.2 ± 1.4 ***
3	17.4 ± 1.9	58.9 ± 6.0 ***	>20	46.5 ± 6.2 **
LY294002	1.9 ± 0.8	88.7 ± 1.5 ***	2.9 ± 0.1	79.5 ± 2.0 ***

Results are presented as mean \pm S.E.M. ($n = 3$). ** $p < 0.01$, *** $p < 0.001$ compared with the control value (DMSO).

^a Concentration required for 50% inhibition (IC_{50}). ^b Percentage of inhibition (Inh %) at 20 μ M.

3. Materials and Methods

3.1. General Experimental Procedures

Measurements of optical rotations, IR, and circular dichroisms spectra were performed on the JASCO P-1020 polarimeter, FT/IR-4100 infrared spectrophotometer (JASCO Corporation, Tokyo, Japan), and Jasco J-715 CD spectrometer, respectively. LRESIMS were measured on a Bruker APEX II (Bruker, Bremen, Germany) mass spectrometer, and HRESIMS were measured on the Bruker APEX II and the Impact HD Q-TOF mass spectrometers (both Bruker, Bremen, Germany). The NMR experiments were recorded on a Varian Unity INOVA 500 FT-NMR (Varian Inc., Palo Alto, CA, USA). The silica gel (40–63 μm , Merck, Billerica, MA, USA) and reversed-phase silica gel (RP-18, 40–63 μm , Merck, Darmstadt, Germany) were used for column chromatography. The thin-layer chromatography (TLC) analysis was carried out on aluminum plates coated with silica gel (Silica gel 60 F254, 100 μm , Merck, Darmstadt, Germany) or C18 gel (Silica gel 60 RP-18 F₂₅₄S, 100 μm , Merck, Darmstadt, Germany). High-performance liquid chromatography (HPLC) was performed on a Hitachi L-2455 HPLC apparatus (Hitachi, Tokyo, Japan) with a Supelco C18 column (250 \times 21.2 mm, 5 μm , Supelco, Bellefonte, PA, USA).

3.2. Animal Material

The marine organism *Spongia* sp. was collected off the Red Sea coast of Jeddah, Saudi Arabia (21°22'11.08" N, 39°06'56.62" E) in March 2016. The biological sample (RSS-1) was stored at the Department of Pharmacognosy, College of Pharmacy, King Saud University, Saudi Arabia.

3.3. Extraction and Separation

The sample of *Spongia* sp. (550 g dry wt) was freeze-dried, chopped, and exhaustively extracted with EtOAc/MeOH/CH₂Cl₂ (1:1:0.5). The combined crude extract was suspended in water, and then partitioned in order with CH₂Cl₂, EtOAc, and *n*-BuOH to obtain CH₂Cl₂ (18.47 g), EtOAc (0.78 g), and *n*-BuOH (1.0 g) fractions, respectively. The CH₂Cl₂ fraction was chromatographed to yield 12 fractions (F1–F12) as described previously [13].

Fraction F7 (1.505 g, 75 % EtOAc/*n*-hexane) was separated by chromatography using an RP-18 column with the elution of H₂O in MeOH (100% to 0%, stepwise) to afford eight subfractions (F7-1 to F7-8). Subfraction F7-3 (146.3 mg, 75 % MeOH/H₂O) was further chromatographed to give ten subfractions (F7-3-1 to F7-3-10) by RP-18 HPLC (50 % MeOH/H₂O). F7-3-4 (17.6 mg) was finally purified to isolate **3** (3.5 mg) by RP-18 HPLC (20% CH₃CN/H₂O). Moreover, F7-3-5 (22.7 mg) was purified to afford **1** (2.4 mg) and **2** (2.0 mg) by RP-18 HPLC (23% CH₃CN/H₂O).

3.3.1. Spongenolactone A (**1**)

White powder, $[\alpha]_D^{25} +37.0$ ($c = 0.24$, CH₃OH); IR (neat) ν_{max} 3444, 2922, 2851, 1747, 1683, and 1653 cm⁻¹; ¹H NMR and ¹³C data, see Table 1; HRESIMS m/z 385.1623 [M + Na]⁺ (calcd for C₂₀H₂₆O₆Na, 385.1622).

3.3.2. Spongenolactone B (**2**)

White powder, $[\alpha]_D^{25} +32.6$ ($c = 0.20$, CH₃OH); IR (neat) ν_{max} 3421, 2919, 2849, 1747, 1684, and 1655 cm⁻¹; ¹H NMR and ¹³C data, see Table 1; HRESIMS m/z 401.1573 [M + Na]⁺ (calcd for C₂₀H₂₆O₇Na, 401.1571).

3.3.3. Spongenolactone C (**3**)

White powder, $[\alpha]_D^{25} +39.0$ ($c = 0.35$, CH₃OH); IR (neat) ν_{max} 3445, 2919, 2849, 1747, 1683, and 1646 cm⁻¹; ¹H NMR and ¹³C data, see Table 1; HRESIMS m/z 379.1750 [M + H]⁺ (calcd for C₂₀H₂₇O₇, 379.1751).

3.4. DFT and TD-DFT Calculations

The DFT approach at the B3LYP/6-31G (d,p) level of theory was applied to simulate the preliminary geometry optimization of conformers [16]. Then, the time-dependent DFT (TD-DFT) approach at the CAM-B3LYP/6-311+G(d,p) level of theory was used to simulate ECD spectra [16]. The integral equation formalism polarizable continuum (IEFPCM) solvent model for MeOH was used for the bulk solvent effect, with all programs calculated by the Gaussian 09 program [17]. The final ECD curves were transformed by GaussSum 2.2.5 and illustrated by Microsoft Excel.

3.5. Cytotoxicity Assay

The cytotoxicity assay was performed using the methods described previously [18,19]. Huh7 cells were used in resazurin assay (Cayman Chemical) and treated with indicated concentrations (12.5, 50.0, and 200.0 μM) of compounds for 72 h. The DMSO control was assigned 100% of relative cell viability. The positive control, Sorafenib, inhibited the 52% growth of Huh7 cells at 12.5 μM .

3.6. Antibacterial Assay

The antibacterial assay was performed using the methods described previously [23]. The bacteria *S. aureus* were cultured in LB (Lysogeny broth) medium in the shaker incubator at 37 °C for 24 h. The bacterial culture was diluted to an absorbance of 0.04 at 600 nm using a sterile LB medium. Tested compounds (cpd) were then added to bacteria aliquots (100 μL /well of 96-well) with the concentrations at 50 μM , 100 μM , and 200 μM , respectively. Background control (1% DMSO in LB solution), positive control (1% DMSO in the diluted bacteria solution), and known drug control (tetracyclin; concentration is 0.5 $\mu\text{g}/\text{mL}$) were run on the same plate. The absorbance at 600 nm (A) was measured right after the testing compounds were added for the basal absorbance and after 16 h incubation at 37 °C. The percentage bacterial growth was calculated as follows: $[(\text{Acpd} - \text{Acpd_basal}) - \text{Abackground control}] / [(\text{Apositive control} - \text{Apositive control_basal}) - \text{Abackground control}] \times 100$.

3.7. Anti-Inflammatory Activity

The dextran sedimentation, Ficoll–Hypaque gradient centrifugation, and hypotonic lysis were used to enrich the neutrophils which were isolated from the blood of healthy adult volunteers, and these methods were described in a previous paper [22]. The neutrophils were incubated in Ca^{2+} -free HBSS buffer (pH 7.4, ice-cold).

Inhibition of Superoxide Anion Generation

Neutrophils (6×10^5 cells/mL) incubated in HBSS (with 0.6 mg/mL ferricytochrome *c* and 1 mM Ca^{2+} , pH 7.4) at 37 °C were treated with the DMSO (as a control) or the tested compounds for 5 min. Neutrophils were activated by 100 nM fMLF for 10 min in the pretreatment of cytochalasin B (CB, 1 $\mu\text{g}/\text{mL}$) for 3 min (fMLF/CB). The generation of superoxide anion was spectrophotometrically measured at 550 nm (U-3010, Hitachi, Tokyo, Japan) [20,21]. LY294002 [2-(4-morpholinyl)-8-phenyl-1(4*H*)-benzopyran-4-one] was used as a positive control.

Inhibition of Elastase Release

Neutrophils (6×10^5 cells/mL) incubated in HBSS (with 100 μM MeO-Suc-Ala-Ala-Pro-Val-*p*-nitroanilide and 1 mM Ca^{2+}) at 37 °C were treated with DMSO (as a control) or the tested compound for 5 min. Neutrophils were activated with fMLF (100 nM)/CB (0.5 $\mu\text{g}/\text{mL}$) for 10 min. The generation of elastase release was spectrophotometrically measured at 405 nm (U-3010, Hitachi, Tokyo, Japan) [21].

4. Conclusions

Three new 5,5,6,6,5-pentacyclic spongian diterpenes, spongenolactones A–C (1–3), were isolated from a Red Sea sponge, *Spongia* sp. These metabolites are the first 5,5,6,6,5-pentacyclic spongian diterpenes bearing a β -hydroxy group at C-1. In our previous chem-

ical study of the same organism, we also discovered a compound of the same skeleton, 17-dehydroxyponalactone, which was found to potently reduce the superoxide anion generation and elastase release [12]. Compounds 1–3 exhibited inhibitory activity against the generation of superoxide anion, and 2 also displayed inhibitory activity against elastase release. Furthermore, 1 showed significant inhibition on the growth of *S. aureus*.

Supplementary Materials: The following supporting information can be downloaded at: <https://www.mdpi.com/article/10.3390/md20080498/s1>, Table S1. The cartesian coordinates of conformer 1, Table S2. The cartesian coordinates of conformer 2, Table S3. The cartesian coordinates of conformer 3, Table S4. The cartesian coordinates of conformer 3c, Table S5. Cytotoxicity (ED₅₀ µg/mL) of compounds 1–3, Figures S1–S26: HRESIMS spectra and 1D and 2D NMR spectra of compounds 1–3.

Author Contributions: Conceptualization and guiding the experiment, J.-H.S.; investigation, C.-J.T., A.F.A. and J.-H.S.; analysis, C.-J.T. and J.-H.S.; writing—original draft, C.-J.T. and J.-H.S.; writing—review and editing, C.-J.T., A.F.A., C.-H.C. and J.-H.S.; technical support for computational software and methodology, C.-H.C. and F.-R.C.; bioactivity assays, C.-H.Y. and T.-L.H.; collection of marine sponge, A.F.A.; species identification, Y.M.H. All authors have read and agreed to the published version of the manuscript.

Funding: The authors are grateful for the financial support from the National Sun Yat-sen University-Kaohsiung Medical University Joint Research Projects (NSYSUKMU 109-I002 and 110-P016) and the Ministry of Science and Technology (MOST 108-2320-B-110-003-MY2 and 110-2320-B-110-001) of Taiwan awarded to J.-H.S.

Institutional Review Board Statement: The study was conducted in accordance with the Declaration of Helsinki. The research protocol was approved by the Institutional Review Board of Chang Gung Medical Hospital (IRB No:201902217A3C601, 24 December 2020). Blood samples were provided by healthy volunteers who signed the written informed consent.

Informed Consent Statement: All subjects gave their informed consent for inclusion before the blood donation.

Data Availability Statement: Data of the present study are available in the article and Supplementary Materials.

Acknowledgments: The authors are thankful to Chao-Lien Ho, Hsiao-Ching Yu, and the Instrumentation Center (MOST 110-2731-M-110-001) at National Sun Yat-sen University, Kaohsiung, Taiwan for the measurement of NMR and MS data; Sheng-Cih Huang and the Center for Advanced Instrumentation and Department of Applied Chemistry (MOST 111-2731-M-A49-001) at National Yang Ming Chiao Tung University, Hsinchu, Taiwan for measurement of MS data; and the Natural Product Libraries and High-Throughput Screening (NPS) Core at Kaohsiung Medical University, Kaohsiung, Taiwan, for high-throughput screening and technical support. The NPS Core is funded by the National Core Facility for Biopharmaceuticals (NCFB) (MOST 110-2740-B-037-001).

Conflicts of Interest: The authors declare no conflict of interest.

References

1. Carroll, A.R.; Copp, B.R.; Davis, R.A.; Keyzers, R.A.; Prinsep, M.R. Marine natural products. *Nat. Prod. Rep.* **2021**, *38*, 362–413. [[CrossRef](#)] [[PubMed](#)]
2. Maximo, P.; Ferreira, L.M.; Branco, P.; Lima, P.; Lourenco, A. The role of *Spongia* sp. in the discovery of marine lead compounds. *Mar. Drugs* **2016**, *14*, 139. [[CrossRef](#)] [[PubMed](#)]
3. Chen, Q.; Mao, Q.; Bao, M.; Mou, Y.; Fang, C.; Zhao, M.; Jiang, W.; Yu, X.; Wang, C.; Dai, L.; et al. Spongian diterpenes including one with a rearranged skeleton from the marine sponge *Spongia officinalis*. *J. Nat. Prod.* **2019**, *82*, 1714–1718. [[CrossRef](#)] [[PubMed](#)]
4. Liang, Y.-Q.; Liao, X.-J.; Lin, J.-L.; Xu, W.; Chen, G.-D.; Zhao, B.-X.; Xu, S.-H. Spongiains A–C: Three new spongian diterpenes with ring A rearrangement from the marine sponge *Spongia* sp. *Tetrahedron* **2019**, *75*, 3802–3808. [[CrossRef](#)]
5. Liang, Y.Q.; Liao, X.J.; Zhao, B.X.; Xu, S.H. (+)- and (–)-Spongiterpene, a pair of new valerenane sesquiterpene enantiomers from the marine sponge *Spongia* sp. *Nat. Prod. Res.* **2019**, *35*, 2178–2183. [[CrossRef](#)]
6. Liang, Y.Q.; Liao, X.J.; Zhao, B.X.; Xu, S.H. Novel 3,4-*seco*-3,19-dinorspongian and 5,17-epoxy-19-norspongian diterpenes from the marine sponge *Spongia* sp. *Org. Chem. Front.* **2020**, *7*, 3253–3261. [[CrossRef](#)]
7. Yang, I.; Lee, J.; Lee, J.; Hahn, D.; Chin, J.; Won, D.H.; Ko, J.; Choi, H.; Hong, A.; Nam, S.-J.; et al. Scalalactams A–D, scalarane sesterterpenes with a γ -lactam moiety from a Korean *Spongia* sp. marine sponge. *Molecules* **2018**, *23*, 3187. [[CrossRef](#)]

8. Ito, T.; Nguyen, H.M.; Win, N.N.; Vo, H.Q.; Nguyen, H.T.; Morita, H. Three new sesquiterpene aminoquinones from a Vietnamese *Spongia* sp. and their biological activities. *J. Nat. Prod.* **2018**, *72*, 298–303. [[CrossRef](#)]
9. Abdjul, D.B.; Yamazaki, H.; Kanno, S.I.; Wewengkang, D.S.; Rotinsulu, H.; Sumilat, D.A.; Ukai, K.; Kapojos, M.M.; Namikoshi, M. Furanoterpenes, new types of protein tyrosine phosphatase 1B inhibitors, from two Indonesian marine sponges, *Ircinia* and *Spongia* spp. *Bioorg. Med. Chem. Lett.* **2017**, *27*, 1159–1161. [[CrossRef](#)]
10. El-Desoky, A.H.; Kato, H.; Tsukamoto, S. Ceylonins G–I: Spongian diterpenes from the marine sponge *Spongia ceylonensis*. *J. Nat. Prod.* **2017**, *71*, 765–769. [[CrossRef](#)]
11. Li, J.; Gu, B.-B.; Sun, F.; Xu, J.-R.; Jiao, W.-H.; Yu, H.-B.; Han, B.-N.; Yang, F.; Zhang, X.-C.; Lin, H.-W. Sesquiterpene quinones/hydroquinones from the marine sponge *Spongia pertusa* Esper. *J. Nat. Prod.* **2017**, *80*, 1436–1445. [[CrossRef](#)]
12. Tai, C.-J.; Huang, C.-Y.; Ahmed, A.-F.; Orfali, R.-S.; Alarif, W.-M.; Huang, Y.M.; Wang, Y.-H.; Hwang, T.-L.; Sheu, J.-H. An anti-inflammatory 2,4-cyclized-3,4-secospongian diterpenoid and furanoterpene-related metabolites of a marine sponge *Spongia* sp. from the Red Sea. *Mar. Drugs* **2021**, *19*, 38. [[CrossRef](#)]
13. Tai, C.-J.; Ahmed, A.F.; Chao, C.-H.; Yen, C.-H.; Hwang, T.-L.; Chang, F.-R.; Huang, Y.M.; Sheu, J.-H. The chemically highly diversified metabolites from the Red Sea marine sponge *Spongia* sp. *Mar. Drugs* **2022**, *20*, 241. [[CrossRef](#)]
14. Zeng, L.-M.; Guan, Z.; Su, J.-Y.; Feng, X.-L.; Cai, J.-W. Two new spongian diterpene lactones. *Acta Chim. Sin.* **2001**, *59*, 1675–1679.
15. Li, C.-J.; Schmitz, F.J.; Kelly-Borges, M. Six new spongian diterpenes from the sponge *Spongia matamata*. *J. Nat. Prod.* **1999**, *62*, 287–290. [[CrossRef](#)]
16. Pescitelli, G.; Bruhn, T. Good computational practice in the assignment of absolute configurations by TDDFT calculations of ECD spectra. *Chirality* **2016**, *28*, 466–474. [[CrossRef](#)]
17. Frisch, M.J.; Trucks, G.W.; Schlegel, H.B.; Scuseria, G.E.; Robb, M.A.; Cheeseman, J.R.; Scalmani, G.; Barone, V.; Mennucci, B.; Petersson, G.A.; et al. *Gaussian 09, revision D.01*; Gaussian Inc.: Wallingford, CT, USA, 2013.
18. Chen, Y.-S.; Chang, H.-S.; Hsiao, H.-H.; Chen, Y.-F.; Kuo, Y.-P.; Yen, F.-L.; Yen, C.-H. Identification of beilschmiedia tsangii root extract as a liver cancer cell–normal keratinocyte dual-selective NRF2 regulator. *Antioxidants* **2021**, *10*, 544. [[CrossRef](#)]
19. Kao, Y.-T.; Chen, Y.-S.; Tang, K.-W.; Lee, J.-C.; Tseng, C.-H.; Tzeng, C.-C.; Yen, C.-H.; Chen, Y.-L. Discovery of 4-anilinoquinolinylchalcone derivatives as potential NRF2 activators. *Molecules* **2020**, *25*, 3133. [[CrossRef](#)]
20. Yu, H.-P.; Hsieh, P.-W.; Chang, Y.-J.; Chung, P.-J.; Kuo, L.-M.; Hwang, T.-L. 2-(2-Fluorobenzamido)benzoate ethyl ester (EFB-1) inhibits superoxide production by human neutrophils and attenuates hemorrhagic shock-induced organ dysfunction in rats. *Free Radic. Biol. Med.* **2011**, *50*, 1737–1748. [[CrossRef](#)]
21. Yang, S.-C.; Chung, P.-J.; Ho, C.-M.; Kuo, C.-Y.; Hung, M.-F.; Huang, Y.-T.; Chang, W.-Y.; Chang, Y.-W.; Chan, K.-H.; Hwang, T.-L. Propofol inhibits superoxide production, elastase release, and chemotaxis in formyl peptide-activated human neutrophils by blocking formyl peptide receptor 1. *J. Immunol.* **2013**, *190*, 6511–6519. [[CrossRef](#)]
22. Hwang, T.-L.; Su, Y.-C.; Chang, H.-L.; Leu, Y.-L.; Chung, P.-J.; Kuo, L.-M.; Chang, Y.-J. Suppression of superoxide anion and elastase release by C18 unsaturated fatty acids in human neutrophils. *J. Lipid Res.* **2009**, *50*, 1395–1408. [[CrossRef](#)] [[PubMed](#)]
23. Jiang, L.W.; Watkins, D.; Jin, Y.; Gong, C.; King, A.; Washington, A.Z.; Green, K.D.; Garneau-Tsodikova, S.; Oyelere, A.K.; Arya, D.P. Rapid synthesis, RNA binding, and antibacterial screening of a peptidic-aminosugar (PA) library. *ACS Chem. Biol.* **2015**, *10*, 1278–1289. [[CrossRef](#)] [[PubMed](#)]